

Selection of the Taylor-Saffman Bubble does not Require Surface Tension

Giovani L. Vasconcelos

*Laboratório de Física Teórica e Computacional, Departamento de Física,
Universidade Federal de Pernambuco, 50670-901, Recife, Brazil.*

Mark Mineev-Weinstein

New Mexico Consortium, Los Alamos, NM 87544, US

(Dated: February 24, 2022)

A new general class of exact solutions is presented for the time evolution of a bubble of arbitrary initial shape in a Hele-Shaw cell when surface tension effects are neglected. These solutions are obtained by conformal mapping the viscous flow domain to an annulus in an auxiliary complex-plane. It is then demonstrated that the only stable fixed point (attractor) of the non-singular bubble dynamics corresponds precisely to the selected pattern. This thus shows that, contrary to the established theory, bubble selection in a Hele-Shaw cell does not require surface tension. The solutions reported here significantly extend previous results for a simply-connected geometry (finger) to a doubly-connected one (bubble). We conjecture that the same selection rule without surface tension holds for Hele-Shaw flows of arbitrary connectivity. We also believe that this mechanism can be found in other, similarly described, selection problems.

Introduction. It is remarkable that numerous processes of pattern formation, ranging from dendritic and fractal growth to viscous fingering and bacterial colony growth, have (after some idealization) the same compact mathematical formulation [1, 2]. Subsequent development of this formulation, called *Laplacian growth*, significantly widened the list of connections by including there 1D-turbulence and generation of complex shapes [3], quantum gravity, integrable systems, random matrices, and conformal theories [4]. The problem of great importance in some processes mentioned above (such as dendritic growth [5] and viscous fingering in a Hele-Shaw cell [6]) was selection of the observed pattern from continuously many solutions.

Background. It has been widely accepted that surface tension is necessary for selecting a single pattern from a continuum of solutions in interface dynamics [7] after it was first conjectured by Saffman and Taylor in 1958 for viscous fingers in a Hele-Shaw cell [6]. Based on their experimental observation these authors argued that as surface tension effects becomes negligible the only one of the set of theoretical finger shapes which can occur is that for which the finger propagates twice as fast as the background flow [6]. But verifying this selection scenario was not possible until much later because of significant mathematical difficulties to include surface tension. After the seminal work of Kruskal and Segur [8], these difficulties were finally resolved, and in the series of works by different groups [9] it was shown that surface tension indeed selects the observed pattern; see also [7] and [10].

More recently, however, it was demonstrated in [11], by using time-dependent exact solutions without surface tension, that contrary to previously mentioned works, selection of the Saffman-Taylor finger is determined entirely by the zero surface tension dynamics. This result calls for a revision of the role of surface tension in pattern selection. But even the simple question of whether selection without surface tension is valid beyond

simply-connected domains (considered in [11]), already presents a mathematical challenge, namely, finding time-dependent exact solutions for multiply-connected Hele-Shaw flows. In the present work we solve this problem for a doubly-connected geometry and significantly extend the results obtained in [11] by addressing the dynamics of a bubble in a Hele-Shaw cell instead of a finger (which is the singular limit of an infinitely long bubble). This extension allows us to conjecture that surface tension (when small enough) is not required for pattern selection in Laplacian growth in domains of arbitrary connectivity.

The pattern selection problem for an inviscid bubble dragged by a viscous flow in a narrow gap between parallel plates (Hele-Shaw cell) was posed by Taylor and Saffman in 1959 [12] and was later addressed experimentally [13] and theoretically [14]. To be specific, the problem was how to select, from the continuum of steady state solutions obtained for zero surface tension, the unique bubble [12] with velocity twice the background flow velocity. While it has long been known that the inclusion of surface tension leads to velocity selection [14], we demonstrate in this paper that the selection mechanism does not require surface tension. Instead, the selection comes about because the selected pattern is the only stable fixed point (attractor) of the non-singular bubble dynamics *without surface tension*.

Problem formulation and plan of the paper. A top-view of a Hele-Shaw channel with lateral walls at $y = \pm\pi$ in our scaled units and with the bubble moving to the right is shown on Fig. 1a. The fluid (oil) velocity obeys the 2D Darcy law, $\mathbf{v} = -\nabla p$, where p is scaled pressure. Far from the bubble the oil flows along the Ox axis with uniform velocity, $V = 1$, thus $p = -x$, when $|x| \rightarrow \infty$. Owing to incompressibility, $\nabla \cdot \mathbf{v} = 0$, p is harmonic, $\nabla^2 p = 0$, in the viscous domain, $D(t)$, where t denotes time. It is thus convenient to introduce a complex potential, $W = \Phi + i\Psi$, where $\Phi = -p$ and Ψ is the stream function. In view of the uniform far-field velocity, one has

$W \approx z$ for $|x| \rightarrow \infty$, so $\Psi = \pm\pi$ at $y = \pm\pi$, since the lateral walls are streamlines. Because pressure is constant (taken to be zero) in the inviscid bubble and continuous across the oil/bubble interface, $\Gamma(t)$, if surface tension is neglected, then $\Phi = 0$ at $\Gamma(t)$. The fluid domain in the W -plane is shown in Fig. 1b, where the vertical slit maps to the interface $\Gamma(t)$ and the rest of the horizontal strip, $-\pi < \Psi < \pi$, to the domain $D(t)$, in the physical plane (Fig. 1a). The kinematic identity, $V_n = v_n$, stating the equality of the normal velocities of the interface, V_n , and of the fluid, v_n , completes the formulation of this free-boundary problem of finding $\Gamma(t)$ given $\Gamma(0)$.

This long-standing nonlinear unstable problem [15] was shown to have an integrable structure and to possess deep connections with other branches of mathematical physics [4]. While numerous exact solutions were obtained for time-dependent interfaces (listed in [16]) and for steady shapes (see [17] and references therein), almost all of them were for simply-connected domains $D(t)$.

Here we present exact solutions for an evolving bubble in a Hele-Shaw cell when the fluid domain $D(t)$ is doubly connected (see Fig. 1a). We then show that these solutions explain not only *how* the moving bubble eventually reaches a stationary shape when $t \rightarrow \infty$, but also *why* the selected bubble moves precisely twice as fast as the background flow when surface tension effects become negligible, in agreement with [13].

In what follows, we first address the dynamics of a bubble with a shape symmetric with respect to the channel centerline. The exact solutions we obtain for this simpler case illustrate our main result, namely, that all non-singular solutions describing bubble shapes converge to the only stable fixed point of this infinitely-dimensional dynamical system, which is precisely the selected member of the continuous family [12]. After that, we extend our solutions to asymmetric bubbles and arrive at the

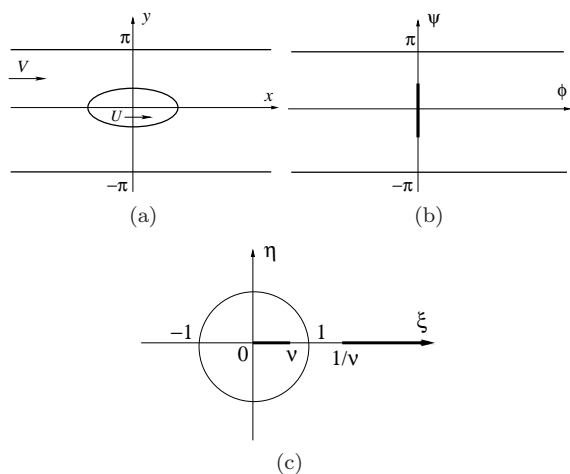


FIG. 1. The fluid domain $D(t)$ for a moving bubble in a Hele-Shaw channel (a), and the corresponding domains in the complex potential plane (b) and in the auxiliary ζ -plane (c).

conclusion that $U = 2$ is still the selected value.

The conformal map and the equation of motion. For a symmetric bubble we introduce a conformal map $z = f(t, \zeta)$ from the exterior of the unit circle with a cut in the complex plane, $\zeta = \xi + i\eta$ (see Fig. 1c), onto the fluid domain, $D(t)$ in the z -plane, $z = x + iy$. The unit circle, $|\zeta| = 1$, maps onto the interface, $\Gamma(t)$, and the cut sides, $\zeta = \xi \pm i0$, where $1 < 1/\nu(t) < \xi < \infty$, map onto the channel walls, $y = \pm\pi$, so that $\zeta = 1/\nu$ and $\xi = +\infty$ are mapped to $x = +\infty$ and $x = -\infty$, respectively. Thus, the polar angle $\phi = \arg(\zeta)$ parametrizes $\Gamma(t)$: $z = f(t, e^{i\phi})$. It is easy to see that the complex potential, $W = \Phi + i\Psi$, satisfying all aforementioned boundary conditions, is

$$W(t, \zeta) = \log \frac{1 - \nu/\zeta}{1 - \nu\zeta}. \quad (1)$$

Rewriting the normal velocity of the interface, V_n , as

$$V_n = V_1 l_2 - V_1 l_1 = \mathcal{I}m(\bar{V}l) = \mathcal{I}m(\bar{z}_t z_s),$$

where $l = l_1 + il_2 = dz/ds$ is the unit tangent vector along the interface, $\Gamma(t) = z(t, s)$, parametrized by an arclength, s , and the subscripts stand for partial derivatives. The normal fluid velocity we rewrite as

$$v_n = \partial_n \Phi = \partial_s \Psi,$$

by virtue of the Cauchy-Riemann condition. Equating the two last formulae, as required by the kinematic identity, and reparametrizing $s \rightarrow \phi$, we obtain $\mathcal{I}m(\bar{z}_t z_\phi) = \Psi_\phi$. Calculating Ψ_ϕ from (1) for $\zeta = e^{i\phi}$, we obtain the equation for the moving interface, $z(t, \phi) = f(t, e^{i\phi})$:

$$\mathcal{I}m(\bar{z}_t z_\phi) = \mathcal{R}e \frac{2\nu}{e^{i\phi} - \nu}. \quad (2)$$

For stationary solutions, $z(t, \phi) = Ut + Z(\phi)$, where the velocity, U , is a constant, equation (2) is simplified:

$$\mathcal{I}m(Z_\phi) = \frac{2\nu}{U} \mathcal{R}e \frac{1}{e^{i\phi} - \nu}. \quad (3)$$

The solution of (3) is the sum of two logarithms:

$$Z = -\log(1 - \nu e^{i\phi}) + \alpha \log(1 - \nu e^{-i\phi}), \quad (4)$$

where the coefficient at the first term equals 1 to satisfy $W = z$ in (1) when $z \rightarrow \infty$. Expression (4) is precisely the one-parameter family of stationary bubbles obtained in [12]. Substituting (4) into (3), we obtain

$$U = \frac{2}{1 + \alpha}. \quad (5)$$

We will show below that all solutions with $\alpha \neq 0$ are unstable and, if perturbed, move to the solution with $\alpha = 0$, which corresponds to $U = 2$, which is the selected value [12, 13].

The finite-parametric solution. Being integrable, equation (2) possesses a rich list of exact solutions, many of

which blow up in finite time. Leaving those aside as physically non-realizable, we present here a rich class of finite parametric *non-singular* solutions (analogous of those obtained earlier [18] for finger dynamics), which remain finite for all times:

$$z = \tau(t) - \log(1 - \nu(t)e^{i\phi}) + \sum_{k=0}^N \alpha_k \log(1 - a_k(t)e^{-i\phi}), \quad (6)$$

where $\alpha_0 = \alpha$ and τ are both real, $a_0 = \nu$, $|a_k| < 1$ for all times, and α_k are constants. These parameters must be chosen so that critical points of the conformal map always stay inside the unit circle to prevent blow ups [19]. Also, the symmetry of the bubble requires that for each term with complex α_k and a_k in the sum there is another term with $\bar{\alpha}_k$ and \bar{a}_k . It is easy to verify that (6) is indeed a solution of (2), where the time-dependence of τ , ν , and a_k is given by the following set of $N + 2$ equations:

$$\beta_k = \tau + \log \bar{a}_k / (\bar{a}_k - \nu) + \sum_{l=0}^N \alpha_l \log(1 - a_l \bar{a}_k), \quad (7a)$$

$$2t + 2t_0 = (1 + \alpha)\tau - \log(1 - \nu^2) + \sum_{k=1}^N \alpha_k \log(1 - \nu a_k), \quad (7b)$$

$$A = (|\alpha|^2 - 1) \log(1 - \nu^2) + \sum_{k=1}^N \sum_{l=1}^N \alpha_k \bar{\alpha}_l \log(1 - a_k \bar{a}_l), \quad (7c)$$

with $k = 1, \dots, N$ in (7a). Here the β_k 's, the initial time t_0 , and the bubble area A are the constants of motion.

The attractor. It follows from (7b) and (7c) that $\tau(t)$ diverges linearly with time, $\tau \rightarrow Ut$, when $t \rightarrow +\infty$. Since β_k is a constant, a real part of at least one logarithm in (7a) should go to $-\infty$ in large times so as to compensate a divergent positive $\tau(t)$. This is possible only if all $a_k(t) \rightarrow 0$ for $k > 0$, as $t \rightarrow \infty$. Thus, we conclude that the origin, $\zeta = 0$, attracts all $a_k(t)$ for $k \geq 1$. Thus, for $t \rightarrow \infty$ the only non-vanishing parameter among the a_k 's is a_0 , which we have identified with ν , meaning that at the initial time we set $a_0(0) = \nu(0)$ and so $a_0(t) = \nu(t)$ for all times. But in this case, the solution (6) asymptotically approaches the family of stationary bubbles (4) discussed above, namely

$$z = \frac{2t}{1 + \alpha} - \log(1 - \nu e^{i\phi}) + \alpha \log(1 - \nu e^{-i\phi}).$$

To test the stability of the trajectory $a_0(t) = \nu(t)$, one has to deviate $a_0(0)$ slightly from $\nu(0)$. One can readily check that the ensuing dynamics for a_0 , ν and τ is given in this case by

$$\begin{aligned} \beta_0 &= \tau + \log \bar{a}_0 / (\bar{a}_0 - \nu) + \alpha \log[(1 - |a_0|^2)(1 - \bar{a}_0^2)], \\ 2(t + t_0) &= \tau - \log(1 - \nu^2) + \alpha \log|1 - a_0 \nu|, \\ A &= -\log(1 - \nu^2) + (\alpha^2/2) \log[(1 - |a_0|^2)|1 - a_0^2]. \end{aligned}$$

These equations clearly show that $a_0 \rightarrow 0$, $\tau \rightarrow 2t$, and $\nu \rightarrow \sqrt{1 - e^{-A}}$ when $t \rightarrow \infty$, so the interface becomes

$$z = 2t - \log(1 - \nu e^{i\phi}). \quad (8)$$

This is precisely the selected pattern with $U = 2$. Thus, $\zeta = \nu$ repels nearby located singularities, which move toward 0. Therefore, the selected bubble, described by (8), represents the only attractor, $\zeta = 0$, of the non-singular subset of the finite-dimensional dynamical systems (6).

The infinite-parametric solution. Let us extend (6) to the case of an infinite number of parameters:

$$z = \tau(t) + \log \frac{1}{1 - \nu(t)e^{i\phi}} + \sum_{k=0}^N \int_0^{a_k(t)} \frac{\rho_k(t, w)}{w - e^{i\phi}} dw, \quad (9)$$

where $a_0 = \nu$ and $|a_k| < 1$ for all k . Solution (9) coincides with (6), if the functions $\rho_k(t, w)$ are constants, and contains all previously known solutions for simply-connected and symmetric doubly-connected cases. (Apparently one can approximate any non-singular solution of (2) by (9), although we have not proved this.) The constants of motion for (9), analogous to β_k in (7), are $B_k = f(1/\bar{a}_k(t))$, which yield [20]

$$B_k = \tau(t) + \log \frac{\bar{a}_k(t)}{1 - \nu(t)\bar{a}_k(t)} + \sum_{l=0}^N \int_0^{a_l(t)} \frac{\rho_l(t, w)}{w - 1/\bar{a}_k(t)} d\zeta,$$

for $k = 1, \dots, N$. A proof, that τ diverges linearly with t , as $t \rightarrow \infty$, and testing the points, ν and 0, for stability is the same as above with the same conclusion, that all $a_k \rightarrow 0$ for $t \rightarrow \infty$, implying that an arbitrary shape, expressed by (9), moves toward the selected bubble (8) with $U = 2$. After having analyzed symmetric bubbles, we now move on to bubbles that are not symmetric with respect to the channel centerline.

Non-symmetric case. The complex potential for a non-symmetric shape requires infinity of reflected images, so we map conformally the annulus, $0 < \sqrt{q} < |\zeta| < 1$, in the ζ -plane (see Fig. 2) onto the fluid domain, $D(t)$, in the z -plane, so that the inner circle, $|\zeta| = \sqrt{q}$, is mapped onto the interface $\Gamma(t)$. The unit circle, $|\zeta| = 1$, is mapped onto the channel walls, $y = \pi$ and $y = 0$. Under reflection with respect to the unit circle (see Fig. 2), we obtain the pre-image of the domain, $\bar{D}(t)$, which is the complex conjugate of the $D(t)$. We map

$$\{\sqrt{q} < |\zeta| < 1/\sqrt{q}\} \rightarrow \{D(t) \cup \bar{D}(t)\},$$

where the annulus $\sqrt{q} < |\zeta| < 1/\sqrt{q}$ is cut along the part of the unit circle, $0 < \arg \zeta < \gamma$, so that the inner (outer) cut side is mapped onto the upper wall (its mirror image), where $y = \Psi = \pm\pi$, while the complimentary arc along the unit circle, $\gamma < \arg \zeta < 2\pi$, is mapped onto the south wall, where $y = \Psi = 0$. We fix the map by sending the points $\zeta = 1$ to $x = +\infty$ and $\zeta = e^{i\gamma}$ to $x = -\infty$.

The complex potential for the non-symmetric case is

$$W(\zeta) = i\gamma/2 + \log \frac{\Theta(e^{-i\gamma}\zeta)\Theta(q\zeta)}{\Theta(qe^{-i\gamma}\zeta)\Theta(\zeta)},$$

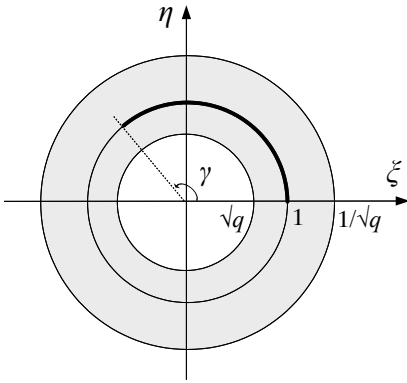


FIG. 2. Flow domain (shaded region) in the ζ -plane for an asymmetric bubble; see text.

where

$$\Theta(\zeta) = (1-\zeta) \prod_{m=1}^{+\infty} (1-q^{2m}\zeta)(1-q^{2m}/\zeta) = \frac{\vartheta_4(\log(\sqrt{\zeta/q}), q)}{\prod_{m=1}^{+\infty} (1-q^{2m})},$$

$$\text{and} \quad \vartheta_4(w, q) = \sum_{n=-\infty}^{\infty} (-1)^n q^{n^2} \exp(2nw)$$

is the Jacobi theta function [21]. It is easy to verify that $W(\zeta)$ satisfies the boundary conditions indicated above.

Finite-parametric solutions for the interface in this case have the form

$$z(t, \phi) = \tau(t) + i\gamma(t)/2 + \log \frac{\Theta(e^{i(\phi-\gamma(t))})}{\Theta(e^{i\phi})} + \sum_{k=1}^N [\alpha_k \log \Theta(a_k(t)e^{-i\phi}) + \bar{\alpha}_k \log \Theta(\bar{a}_k(t)e^{i\phi})]. \quad (10)$$

Here all $|a_k| < 1$, and $\sum_{k=1}^N \alpha_k = 0$. Since y is multiple of π when $|\zeta| = 1$, then τ is purely real. Inserting (10) into (2) and integrating the resulting equations of motion, we obtain $N + 2$ complex constants of motion: $\beta_k = f(t, q/\bar{a}_k)$ for $k = 1, \dots, N$, $\beta_+ = f(t, q)$, and $\beta_- = f(t, qe^{i\gamma})$, where

$$\beta_k = \tau + i\gamma/2 + \log [\Theta(q e^{i\gamma} \bar{a}_k) / \Theta(q \bar{a}_k)] + \sum_{l=1}^N [\alpha_l \log \Theta(a_l \bar{a}_k / q) + \bar{\alpha}_l \log \Theta(q \bar{a}_l / \bar{a}_k)], \quad (11a)$$

$$\beta_{\pm} = \tau - 2t + i\gamma/2 \pm \log [\Theta(q e^{i\gamma}) / \Theta(q)] + \sum_{l=1}^N [\alpha_l \log \Theta(e^{-i\gamma_{\pm}} a_l / q) + \bar{\alpha}_l \log \Theta(q e^{i\gamma_{\pm}} \bar{a}_l)] \quad (11b)$$

where $\gamma_+ = 1$ and $\gamma_- = \gamma$. The constants, β_+ and β_- are not independent, since $\text{Im} \beta_+ = \text{Im} \beta_- = \gamma/2 + \text{Im} \sum_{l=1}^N \alpha_l \log a_l$. The formulae (11) constitute the full dynamics of a_k , γ , q , and τ . The bubble area, A , while

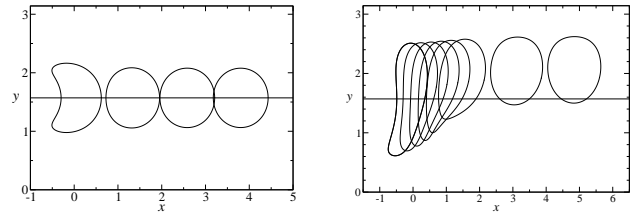


FIG. 3. Examples of bubble evolution: (a) symmetric solution and (b) asymmetric solution.

fixed in time, is not an independent constant of motion; it is neatly expressed through other constants as

$$A/\pi = \beta_+ - \beta_- + 2\mathcal{R}e \sum_{k=1}^N \bar{\alpha}_k \beta_k.$$

The attractor. After eliminating τ from (11a), by subtracting β_+ (or β_-) from β_k , we see that the term, $2t$, in the resulting conserved constant must be canceled by a divergent logarithmic term. This implies that all $a_k \neq q$ must move to the point $qe^{i\gamma}$, when $t \rightarrow \infty$. The points q and $qe^{i\gamma}$ are the repeller and the attractor respectively for the dynamical system expressed by (11). Taken at the limit $t \rightarrow \infty$, these two points are the only fixed points of this system. If one of the a_k 's, say a_1 , was initially at the repeller, $a_1 = q$, then β_1 diverges, and $U = 2/(1 + \alpha_1) \neq 2$, when $t \rightarrow \infty$. After relocating a_1 out of q (by setting $a_1(0) \neq q(0)$), the asymptotic velocity of the bubble reaches the same selected value, $U = 2$, as in the symmetric case.

For $\beta = \pi$, the solution (10) describes symmetric bubbles and thus recovers (6), albeit in a different formulation. A symmetric bubble evolution is shown in Fig. 3a, where the asymptotic shape corresponds to the Taylor-Saffman bubble [12] with $U = 2$, as described by (8). In Fig. 3b we show an asymmetric solution whose asymptotic shape coincides with the asymmetric bubble obtained in [14, 17] for $U = 2$. Notice furthermore that since all a_k move toward the same point, $a_k \rightarrow qe^{i\gamma}$, for $t \rightarrow \infty$, the sum in (11) vanishes because $\sum_{k=1}^N \alpha_k = 0$, so $\gamma(t) \rightarrow \text{Im} \beta_+ = \text{Im} \beta_-$, which is a constant of motion whose value is set by the initial conditions. Thus, it remains to be seen how to centralize a bubble in our framework (if possible at all), so that $\gamma \rightarrow \pi$ as $t \rightarrow \infty$.

For want of space, we do not present here the selection for the asymmetric bubble with infinitely-parametric non-singular solutions, which is the analog of (9). It suffices to say that in this case selection of the bubble velocity $U = 2$ is also achieved in the limit $t \rightarrow \infty$.

The results presented here (and the results of [11] for a finger, which is a singular limit of this work, when $\nu = 1$) unambiguously indicate that the stability of the selected pattern, with respect to the rest of the family, is built in the Laplacian growth *without surface tension*. In this context, surface tension is just one of infinitely many perturbations (perhaps the most relevant) which kicks the

system toward the attractor, while also regularizing high curvatures. The selected pattern, while linearly unstable in the absence of surface tension, is stable asymptotically: if perturbed, it eventually recovers its original shape.

In conclusion, since the selection mechanism in both simply-connected and doubly-connected geometries is due to the attractor for all nonsingular solutions with

zero surface tension, we conjecture that the same holds for Laplacian growth in domains of arbitrary connectivity. We also think that the same selection mechanism can be found in other free boundary problems with the same (or similar) mathematical description .

One of us (M.M-W) thanks MPIPKS (Dresden) and UPFE (Recife) for hospitality when this work was done.

-
- [1] J. S. Langer, Rev. Mod. Phys. **52**, 1 (1980).
 [2] D. Bensimon et al., Rev. Mod. Phys. **58**, 977 (1986).
 [3] M. B. Hastings, L. S. Levitov, Physica D **116**, 244 (1998).
 [4] M. Mineev-Weinstein, P. B. Wiegmann, and A. Zabrodin, Phys. Rev. Lett. **84**, 5106 (2000).
 [5] G. P. Ivantsov, Dokl. Akad. Nauk. SSSR **58**, 567 (1947).
 [6] P.G. Saffman and G. I. Taylor, Proc. R. Soc. Lond. A **245**, 312 (1958).
 [7] P. Pelcé, *Dynamics of Curved Fronts* (Academic Press, San Diego, 1988).
 [8] M. D. Kruskal and H. Segur, Stud. Appl. Math. **85**, 129 (1991).
 [9] B.I. Shraiman, Phys. Rev. Lett. **56**, 2028 (1986); D.C. Hong and J.S. Langer, Phys. Rev. Lett. **56**, 2032 (1986); R. Combescot et al., Phys. Rev. Lett. **56**, 2036 (1986); S. Tanveer, Phys. Fluids **30**, 1589 (1987).
 [10] D. A. Kessler, J. Koplik and H. Levine, Adv. Phys. **35**, 255 (1988); H. Segur, S. Tanveer and H. Levine (eds.), *Asymptotics Beyond All Orders* (Plenum Press, New York, 1991).
 [11] M. Mineev-Weinstein, Phys. Rev. Lett. **80**, 2113 (1998).
 [12] G. I. Taylor and P. G. Saffman, Q. J. Mech. Appl. Maths **12**, 265–279 (1959).
 [13] A. R. Kopf-Sill and G. M. Homsy, Phys. Fluids **31**, 18 (1988), T. Maxworthy, J. Fluid Mech. **173**, 95 (1986). S. Shad et al., J. of Petrol. Sci. and Eng. **72**, 67–77 (2010).
 [14] S. Tanveer, Phys. Fluids **30**, 651 (1987)
 [15] A comprehensive bibliography on the subject up to 1998: <http://people.maths.ox.ac.uk/howison/Hele-Shaw>.
 [16] B. Gustafsson and A. Vasil'ev, *Conformal and Potential Analysis in Hele-Shaw Cell* (Birkhäuser, Basel, 2006); M. Mineev-Weinstein, M. Putinar, R. Teodorescu, J. Phys. A **41** 263001 (2008).
 [17] G. L. Vasconcelos, J. Fluid Mech. **444**, 175 (2001).
 [18] M. Mineev-Weinstein and S. P. Dawson, Phys. Rev. E **50**, R24 (1994); S. P. Dawson and M. Mineev-Weinstein, Physica (Amsterdam) **73D**, 373 (1994).
 [19] One should also stay away from initial data leading to the loss of univalence of the interface. It is easy to accommodate, and we do not discuss details here.
 [20] The rest of formulae related to the solution (9) will be presented elsewhere.
 [21] I. S. Gradshteyn and I. M. Ryzhik, Table of Integrals, Functions, and Products, (1980) Acad. Press, London.